CEBAF Program Advisory Committee Six (PAC6) Proposal Cover Sheet

This proposal must be received by close of business on April 5, 1993 at:

Roy Whitney, CEBAF
User Liaison Office
12000 Jefferson Avenue
Newport News, VA 23606

Proposal Title

Studies of the (e,e'p) Reaction at High Missing Energy

Contact Persons

Name: W. Bertozzi, J.P. Chen, S. Gilad
Institution: Massachusetts Institute of Technology
Address: Lab. for Nuclear Science
Address: 77 Massachusetts Ave.
City, State ZIP/Country: Cambridge, MA 02139
Phone: (617) 253-5167 **FAX:** (617) 258-5440
E-Mail → BITnet: Bertozzi@MITLNS **Internet:** BERTOZZI@MITLNS.MIT.EDU

If this proposal is based on a previously submitted proposal or letter-of-intent, give the number, title and date:

No.

CEBAF Use Only

Receipt Date: 4/5/93 Log Number Assigned: PR 93-048

By: gp

Studies of the (e,e'p) Reaction at High Missing Energy

W. Bertozzi, J.P. Chen, D. Dale, S. Gilad, A. Sarty

Massachusetts Institute of Technology, Cambridge, MA 02139

A. Saha, P. Ulmer

CEBAF, Newport News, VA 23606

L. Weinstein

Old Dominion University, Norfolk, VA 23529

D. Kawall, Z.E. Meziani

Stanford University, Stanford, CA 94305

R. Lourie

University of Virginia, Charlottesville, VA 22901

M. Finn

College of William and Mary, Williamsburg, VA 23187

And the Hall A Collaboration.

Spokesmen: W. Bertozzi, J.P. Chen, D. Dale, S. Gilad, A. Sarty

Abstract

We propose to make a detailed study of (e,e'p) reactions at high missing energy for selected kinematics. R_L and R_T separations will be performed for ^{12}C at the quasielastic peak for a Q^2 range from 0.2 to 1.5 $(GeV/c)^2$, and also for $^{3,4}He$ at $Q^2 = 1(GeV/c)^2$. Existing (e,e'p) data at high missing energy, especially the transverse response at low q, show excessive strength beyond the one nucleon process. By studying the Q^2 and A dependence, we hope to learn the nature of this phenomenon and the relationship to the (e,e') phenomenology, and therefore to improve our understanding of the nucleon-nucleon interactions as well as two- and multi-nucleon correlations. We will also perform a quick measurement of the energy transfer dependence by measuring cross sections (without L/T separation) at several ω's for ^{12}C at $Q^2 = 1(GeV/c)^2$. We hope to learn more about the contributions from processes other than quasielastic scattering.

I. BACKGROUND AND MOTIVATION

1. INTRODUCTION

Recent studies of the $^{12}C(e,e'p)$ and other (e,e'p) reactions show that the (e,e') reaction in the quasifree region is very complex. It appears that the (e,e') reaction proceeds in part via a simple one-nucleon interaction and in part via two-nucleon and maybe even multi-nucleon components. These two- and multi-nucleon components could be as important as the one-body process and cannot be fully attributed to final state rescattering. They are part of the (e,e') interaction.

Below, we describe the difficulties which exist with our understanding of the (e,e') reaction. We also present evidence for what appears to be multi-hadron processes. We emphasize evidence from the (e,e') and (e,e'p) reactions, but we note also observations from measurements in other fields of nuclear physics which could very well be related. These include photo- and pion absorption. At present, conventional theories are unable to properly account for these results. Regardless of the origin of these phenomena, it is clear that they are not well understood. Systematic experimental work is needed if we are to have any chance of theoretical understanding. For the case of electron scattering, CEBAF is the natural place to investigate the systematics of these phenomena. Indeed, efforts directed at the detection of multi-hadrons is planned for CLAS. However, certain important aspects of the reaction can be measured only in Hall A. These include the separated (e,e'p) responses (particularly at deep missing energies where the cross sections are small), and their systematic dependence on Q^2, nuclear density, and nucleon initial

momentum. It is striking that there exists only one measurement of these separated responses. The quality of the data that can be obtained in Hall A will be far superior to existing data, even those at low Q^2. Extension of these measurements to higher Q^2 is only possible at CEBAF.

2. PROBLEMS WITH THE QUASIFREE PICTURE OF (e,e')

Measurements of unseparated inclusive (e,e') cross sections support the traditional microscopic view of the nucleus as a collection of protons and neutrons in a mean field[1]. Moreover, the (e,e') process on a range of nuclei[2]was characterized by quasifree scattering from a Fermi gas of N neutrons and Z protons with two parameters, the Fermi momentum and a shift in the energy transfer. Closer examination of the (e,e') data reveals problems with the one-body interpretation. First, the large cross section in the dip region between the quasielastic and the Δ bumps cannot be accounted for by the tails of these two peaks. Meson exchange currents can explain only part of this excess cross section[3]. A second difficulty with the simple quasifree description is encountered by the separation of the longitudinal and transverse responses. Figures 1 and 2 display the transverse and longitudinal scaling functions, $f_T(y)$ and $f_L(y)$ respectively, for ^{12}C(e,e')[4]and for ^{3,4}He(e,e')[5], where y is the relativistic scaling variable. These data involve many momentum transfers. The scaling functions $f_L(y)$ and $f_T(y)$ do scale separately. However, if the process were truly quasifree, $f_L(y)$ and $f_T(y)$ should be equal for $y \leq 0$ where the tail of the Δ is known to be inconsequential. As can be seen in Figures 1 and 2, they are not equal for ^{4}He and ^{12}C, indicating that the quasifree assumption is not justified by the data. This difference between $f_L(y)$ and $f_T(y)$ persists for all nuclei larger than ^{3}He and can be even larger than that in ^{12}C. It is also of interest to notice that at high momentum transfer ($q > 1$ GeV/c), the difference between $f_L(y)$ and $f_T(y)$ at negative y persists for heavy nuclei[6], while for ^{4}He the difference seems to vanish[7]. A third indication that the (e,e') process in the quasielastic region is considerably more complex than implied by the quasifree model is given by the comparison between the data and the Coulomb sum rule. The Coulomb sum is the integral of the longitudinal response function divided by the single nucleon form factor at fixed q over all ω. In the nonrelativistic impulse approximation at large enough q, the Coulomb sum should approach Z, the number of protons. For $A > 4$, it is typically 20% too small[8].

Many theoretical attempts were made to explain the separated response functions, ranging from the Dirac σ - ω model[9], final state interactions[10], off-shell effects[11]to various nucleon modifications[12]. None of the single particle models reproduces both the longitudinal and the transverse response functions.

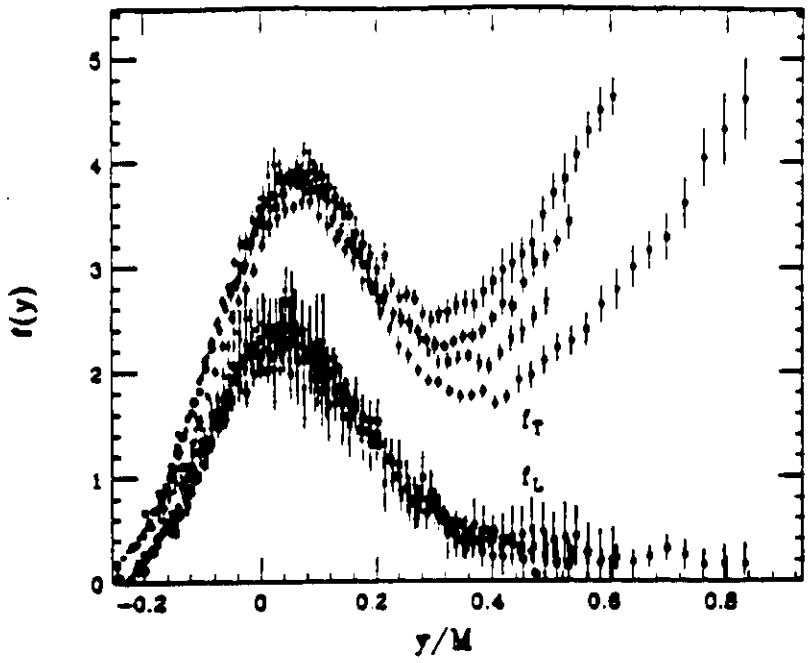

Figure 1. Longitudinal and transverse scaling functions in $^{12}C(e,e')^4$ *for momentum transfers of 400, 450, 500, 550 and 600 MeV/c.*

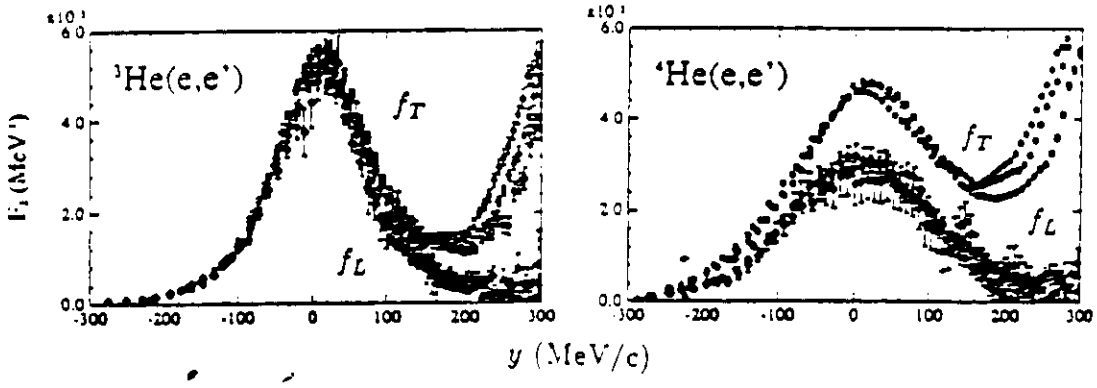

Figure 2. Longitudinal and transverse scaling functions in $^{3,4}He$ *for* $400 < q < 600$ *MeV/c.*[5]

3. COINCIDENCE CROSS SECTIONS: (e,e'p)

A series of ^{12}C(e,e'p) coincidence experiments at Bates studied the nature of the (e,e'p) reaction. All of these experiments were performed in parallel kinematics at a variety of energy and momentum transfers.

Figure 3 shows the longitudinal and transverse $^{12}C(e,e'p)$ response functions, R_T and R_L, at q = 400 MeV/c and ω = 120 MeV[13]. It also shows the difference in the spectral functions, $S_T - S_L$. These were measured very close to the maximum of the quasielastic peak corresponding to y $\gtrsim$ 0. Under these conditions one would expect that the one-body process would dominate. Several features stand out:

1) The p-shell strength (^{11}B ground state) is all in one point of the histogram at a missing energy of about 17.5 MeV. For this transition the transverse and longitudinal spectral functions are almost equal ($S_T - S_L \approx 0$) as one would expect since the free nucleon form factors have been divided out of the R's. This is the behavior one expects of a quasifree process.

2) The longitudinal response, R_L, shows a broad s-shell peak, about 15 MeV FWHM, located at a missing energy of about 38 MeV. Above 48 MeV R_L is consistent with zero. This is reasonable for a mean field or shell model. The width is consistent with deep hole states corresponding to high excitations and thus short lifetimes. These highly excited s-shell hole states will decay predominantly by nucleon emission. This kind of two-nucleon emission should not be confused with a two-body correlation that leads to the two-body process.

3) The transverse response, R_T, also shows a bump at about 38 MeV of missing energy. In contrast to R_L, R_T is not localized in missing energy. R_T remains large out to 65 MeV, the largest missing energy measured. If the (e,e'p) process were quasifree, then R_L and R_T would have the same shape. This R_L/R_T difference is not likely due to final state rescattering in the sense of a cascade model calculation[18]. The transverse strength at large missing energy (E_m > 48 MeV) may be characteristic of a non-quasifree process.

4. The difference between the spectral functions, S_T - S_L, shown in the bottom of Figure 3, starts growing at 28 MeV, the threshold for two-nucleon emission, and extends beyond 65 MeV. The threshold behavior is confirmed by results from NIKHEF[14]. The transverse/longitudinal ratio for ^{6}Li also starts increasing at the two-nucleon threshold[15]. If the process were quasifree, the difference in spectral functions would be zero.

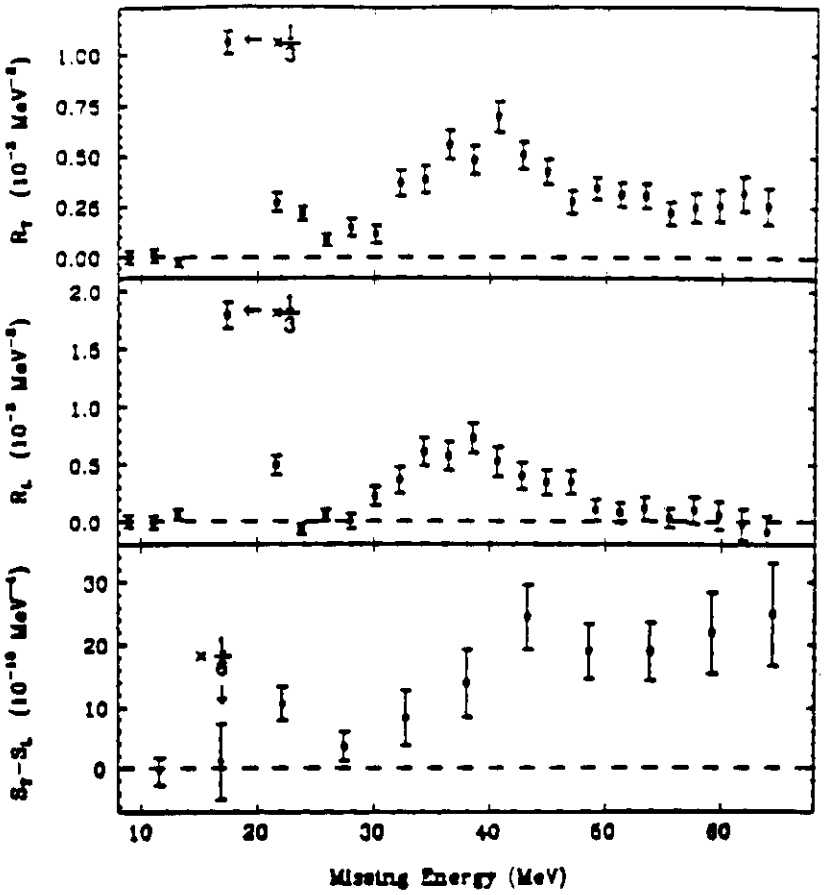

Figure 3. Separated $^{12}C(e,e'p)$ response functions and their difference for kinematics near the quasielastic peak: q = 400 MeV/c and ω = 120 MeV[13]. Transverse (top) and longitudinal (middle) response functions and the difference in the spectral functions (bottom) vs. missing energy.

It is not unreasonable to conclude that these differences might originate from a new process, transverse in nature, that involves at least two nucleons.

A similar phenomenon is seen in the dip region, where strength is observed at missing energies as high as 160 MeV.[16]. Even in the Δ-region the ^{12}C(e,e'p) missing energy spectra exhibit indications of two-nucleon processes[17]. The data support the conclusion that the two-nucleon process is not dominated by the quasifree delta production with $\Delta + N \rightarrow N + N$.

Results of ^{12}C(e,e'p) experiments on the quasielastic peak performed at higher mo-

mentum transfers in parallel kinematics are shown in Figure 4 [18,19]. These data were taken at relatively large scattering angles and at high momentum transfers so that they are predominantly transverse. The p- and s-shell peaks are seen clearly and once again an appreciable high missing energy tail is seen. The high missing energy strength cannot be generated by one-body processes with final state rescattering[18]. The strength from this rescattering becomes negligible above about 80 MeV.

The behavior of the high missing energy strength is shown on Figure 5 for three regions: $50 \leq E_m \leq 150$ MeV , $50 \leq E_m \leq 80$ MeV and $50 \leq E_m \leq 350$ MeV. The plot shows the ratio of the strength in these regions to the (e,e'p) strength below 50 MeV, which we consider the quasifree or one-body yield. Recall, however, that the additional transverse strength really begins at 28 MeV, the 2N threshold. At the quasielastic peak one would have expected the best agreement with the quasifree picture of the (e,e') process. Yet, as seen in Figure 5, even at the quasielastic peak we observe many-body effects that increase with q and with ω and that are more than 40% of the (e,e'p) and thus of the (e,e') process.

Figure 6 shows the ω dependence of $^{12}C(e,e'p)$[19]at $q = 900 \rightarrow 1000$ MeV/c. The bottom graph, at $\omega = 475$ MeV, corresponds to a recoil momentum near zero. The middle graph, at $\omega = 330$ MeV, corresponds to a recoil momentum near -150 MeV/c. The top graph, at $\omega = 240$ MeV, corresponds to a recoil momentum of ≈ -200 MeV/c. It is clear that the strength at high missing energies decreases dramatically with decreasing ω. From the data presented this far it might be concluded that there are two- or many-nucleon processes which are observed in the $^{12}C(e,e'p)$ reaction. They are transverse in nature and are manifested as excess strength in deep missing energies. The signature and characteristics are as follows:

Missing Energy (MeV)	Contributing Processes
14 – 28	$1p_{3/2}$ Single-Particle knockout: $S_L/S_T \sim 1$
28 – 48	$1s_{1/2}$ Single-Particle Knockout Two-Particle Knockout: $S_L/S_T < 1$
48 – 150	Two-Particle Knockout Multi-Particle Knockout? $S_L/S_T < 1$
> 150	Real Pion Production: $S_L/S_T < 1$ Multi-Particle Knockout?

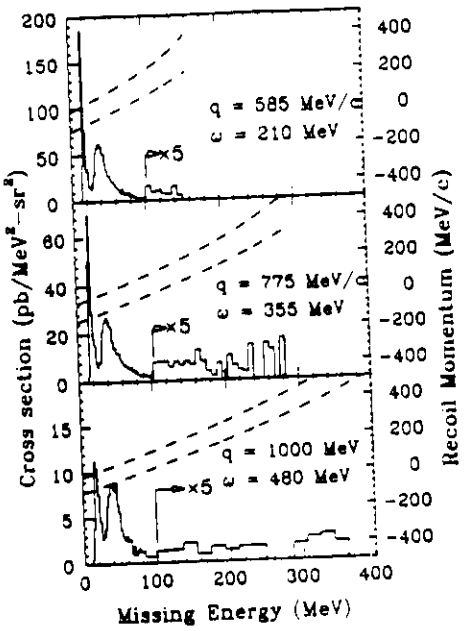

Figure 4. $^{12}C(e,e'p)$ *cross section near the quasielastic peak. Top two figures from Weinstein et al*[19]. *Bottom figure from Morrison et al* [20]. *The right hand scale refers to the dashed curves showing the acceptance in recoil momentum.*

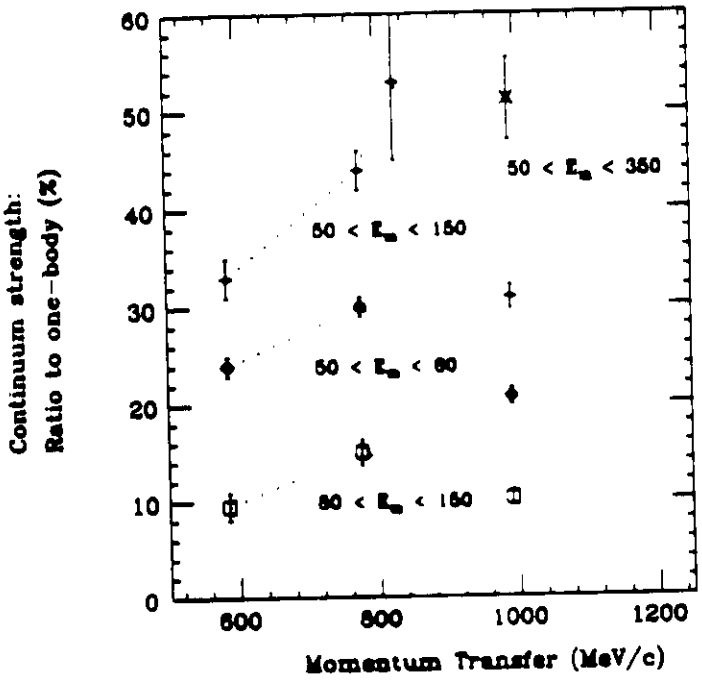

Figure 5. Ratio of Continuum Strength to Single-Nucleon Strength[19]. *The single-nucleon knockout strength is defined to be in the region* $10 \leq E_m \leq 50$ *MeV. The dotted lines join the points calculated from the same continuum region of missing energy.*

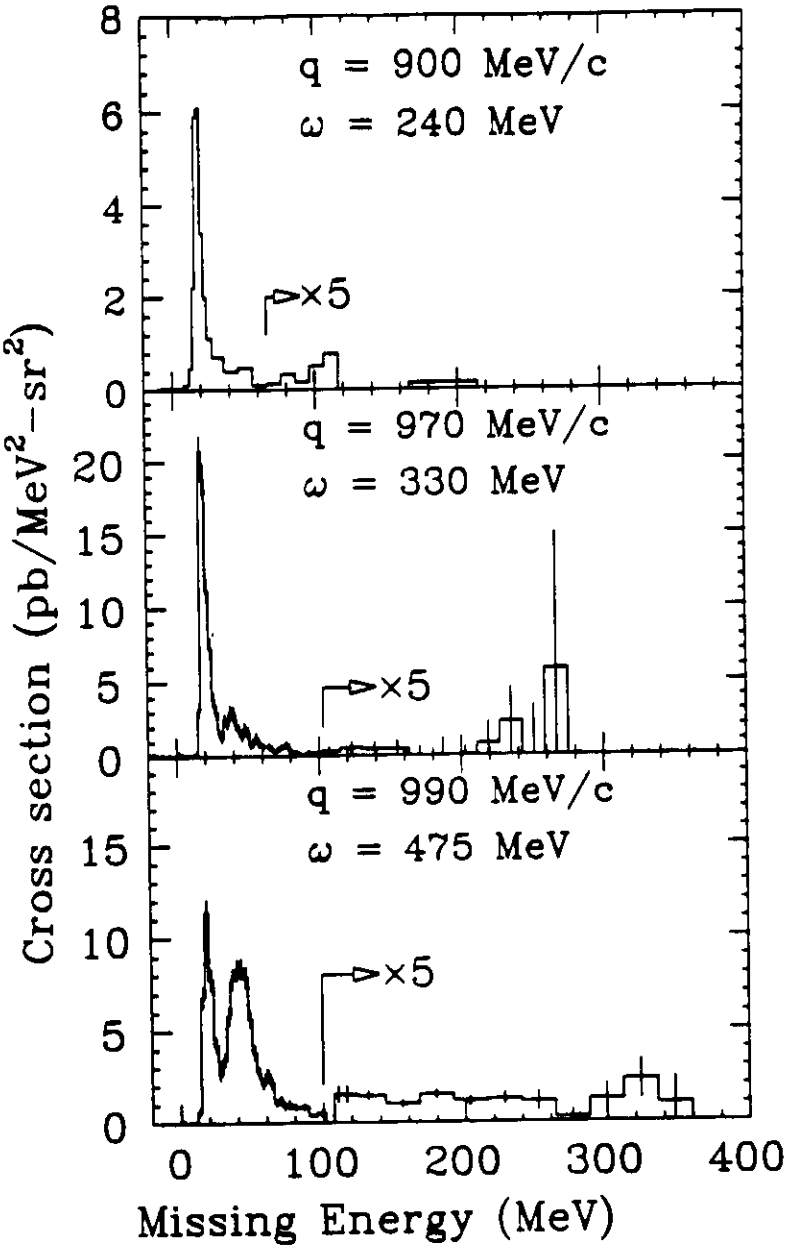

Figure 6. $^{12}C(e,e'p)$ *data comparing missing energy spectra with (e,e') kinematics near the quasielastic peak (bottom),*[19] *approximately halfway down the quasielastic peak (middle),*[19] *and with* ω *corresponding to* $x = 2$ *(top)* [20].

The importance of two-body effects has also been observed in ^{3}He(e,e'p). The data demonstrate both single nucleon knockout and three-body breakup[21]. The centroid of the three-body breakup strength moves to larger missing energy as the missing momentum, P_R, increases. This is suggestive of a picture wherein the large momenta are generated

by back-to-back short range collision of two nucleons, so that the excitation energy is effectively the energy of the recoil partner.

4. OTHER MULTI-NUCLEON PROCESSES

In the following section, some other systems in which multi-nucleon processes are believed to be important will be discussed. Note that in pion and photo-absorption, the dominant mechanism involves two nucleons (quasideuteron absorption) and is relatively well established. Thus, attention is given here to mechanisms involving more than two nucleons.

Theoretical studies of the trinucleon system using numerically exact Faddeev calculations have pointed to effects due to three-nucleon processes. Calculations of the trinucleon binding energies, using various realistic nucleon-nucleon potentials, underbind the trinucleon by approximately 1 MeV. Addition of a modern three-nucleon potential provides the additional required binding[22]. Similar comparison to exact Faddeev calculations indicate that the measured doublet a_2 scattering length for low energy neutron-deuteron scattering can only be accounted for by inclusion of a three-nucleon process. More involved Faddeev calculations of neutron-induced deuteron breakup have been performed and compared to experimental results in selected kinematic configurations[23]. These comparisons show a significant enhancement of the measured cross sections over the predictions in a kinematic configuration (the "symmetric space-star") which is particularly insensitive to the nucleon-nucleon potential model used in the calculations. This deviation has been attributed to the presence of three-nucleon processes.

In pion absorption experiments, effects attributed to multi-nucleon mechanisms have been studied in a more systematic manner, but the theoretical framework for these mechanisms is much less clear. The first signature for pion absorption in which more than two nucleons are involved was the missing strength in the measured two-nucleon absorption process. A pion absorption mechanism involving three-nucleons was first clearly identified[24]in 1985 on ^{3}He. This showed a strong correlation with three-nucleon phase. Since that time, a host of pion absorption experiments have been performed on ^{3}He, ^{4}He and heavier nuclei to study this phenomenon (see ref. [25]and references therein). In the case of ^{4}He, absorption resulting in three- and four-body like phase space was observed[26]. All of these measurements reveal evidence that an appreciable amount of the total absorption cross section (up to 50%) is due to a mechanism that involves three or more nucleons. The nature of this mechanism is currently unknown. However, neither initial nor final state interactions can account for the data and in the three-nucleon case, this process seems to be clearly related to three-nucleon processes[27].

Recent measurements of the three-body photodisintegration of ^{3}He have been performed in selected kinematical regions expected to be dominated by three-nucleon effects. Experiments have been carried out at Saclay[28]with photon energies of 320-450 MeV, and at Saskatoon[29]with photon energies of 150-225 MeV. Both measurements were compared to microscopic photodisintegration calculations which included the effect of absorption by a three-nucleon current[30]. Results over this entire energy range (150-450 MeV) confirm the need to include a three-nucleon mechanism to describe the data taken at these selected kinematics.

Large efforts are underway at laboratories such as PSI, Saskatoon, and Mainz to investigate the multi-hadron aspects of pion and photon absorptions. Mostly, these efforts are based on large solid angle detectors to detect all hadrons resulting from the absorption processes. A similar effort, with the (e,e'nX) reaction is planned at CEBAF using CLAS in Hall B. However, to study the details of these processes requires the coincidence high resolution capabilities available at Hall A. Only Hall A provides the ability to measure the small cross sections seen at deep missing energies and to separate the longitudinal and transverse responses with precision. The striking observation at lower momentum transfer that the strength at high missing energies in ^{12}C(e,e'p) is transverse could not be made without similar capabilities. Any theory dealing with these phenomena will need input such as separated responses, dependence on momentum and energy transfers and dependence on nucleon initial momentum. In this respect, experiments in both Halls A and B should be viewed as necessary and complementary.

II. PROPOSED MEASUREMENTS

The goal of this experiment is to study the systematic behavior of the (e,e'p) reaction at high missing energies (E_m) and to investigate the contributions from possible multinucleon processes. We will mainly focus on the momentum transfer (Q^2) dependence and atomic number (A) dependence. We propose to perform R_L and R_T separations for four Q^2 values ranging from 0.2 to 1.5 (GeV/c)^2 with a ^{12}C target and perform separations at Q^2 of 1 (GeV/c)^2 also on ^{3}He and ^{4}He. Proton momenta are chosen to be parallel to $\vec{q}$, so that only R_L and R_T will contribute. The above measurements will take up most of the requested beam time. We also propose to make a quick ω dependence on ^{12}C study by measuring total cross sections (without L/T separations) on both sides of the quasielastic peak and in the dip and Δ regions at Q^2 of 1 (GeV/c)^2.

In ^{12}C (e,e') as well as ^{12}C (e,e'p), a large amount of low q data shows that the longitudinal and transverse responses are very different. In the lighter nuclei, with only (e,e') data avaliable, the differences in the longitudinal and transverse responses are not as

obvious. Therefore, ^{12}C is chosen for the momentum dependence measurements. For the A dependence study, separations at $Q^2 = 1(GeV/c)^2$ with ^{3}He and ^{4}He are chosen in addition to ^{12}C to emphasize the possible influence of the onset of the longitudinal/transverse anomaly in (e,e').

All of our measurements, except the ω dependence study, will be performed at the quasielastic peak. At quasielastic kinematics, the reaction mechanism is most likely to be clean, *i.e.*, the one-nucleon-knockout assumption is supposed to be valid. However, as has been pointed out earlier, the existing (e,e'p) and (e,e') data indicate that the simple quasifree models do not work well even at the quasielastic peak.

From the Q^2 dependence study, we will put stringent constraints on theoretical models as possible candidates to explain the puzzling extra transverse strength at high missing energy for quasielastic (e,e'p), and also for the missing longitudinal strength in both quasielastic (e,e') and (e,e'p). The Q^2 dependence study can help shed lights on the understanding if the above phenomena are due to relativistic effects and modification of nucleon form factors resulting from partial deconfinement, or due to final state interactions, off-shell effects and correlations.

For ^{3}He(e,e') there does not appear to be a difference in longitudinal and transverse responses. This difference first appears in ^{4}He. Therefore it is important to examine ^{3}He(e,e'p) and ^{4}He(e,e'p), as well as ^{12}C(e,e'p) to investigate the systematic behaviour of (e,e'p) and its relationship to the (e,e') phenomenology. By studying the A dependence (also the density dependence), we may learn if the effects come from the nuclear medium modification of nucleon properties or multinucleon processes. For light nuclei (^{3,4}He), it will be easier to compare experimental results with theories since reasonable theoretical calculations are possible. Therefore it is very useful to make measurements simultaneously with nuclei of different A.

From the ω dependence study, we may learn about the other mechanisms such as meson exchange currents, isobar currents, and possible other multinucleon current contributions.

To achieve the high precision and good energy resolution needed for R_L and R_T separations, the Hall A High Resolution Spectrometers will be used with their standard high quality detector packages. In terms of the capabilities of the Hall A spectrometers for resolution, particle identification, etc., the experiment is well within the design specifications. ^{12}C targets with thickness of 0.1 and 0.4 g/cm^2 and 10 cm long high pressure gas ^{3,4}He targets with thickness of 0.1 g/cm^2 will be used for the measurements. The thickness requirement of our helium targets is about an order of magnitude smaller than the current

design of the Hall A helium targets.

III. KINEMATICS AND COUNT RATE ESTIMATES

The Q^2 dependence study will be done on ^{12}C at Q^2 of 0.2, 0.6, 1 and 1.5 $(GeV/c)^2$ on the quasielastic peak. For the R_L and R_T separations, we will measure cross sections at two electron scattering angles of 15.5° and 90°, (except for Q^2 of 1.5 $(GeV/c)^2$, where we have to go to 19.8° instead of 15.5° because of the beam energy limitation). We will cover the whole missing energy spectrum by sweeping the proton spectrometer field setting at each Q^2 point. Table 1 summarizes the kinematics.

For the A dependence part, additional measurements on $^{3,4}He$ will be performed at a Q^2 of 1 $(GeV/c)^2$ on the quasielastic peak, again covering the whole missing energy spectra. Separation of R_L and R_T will be performed for both targets. The kinematics for the $^{3,4}He$ measurements is listed on Table 2.

The ω dependence study will be performed at 15.5° at a Q^2 of 1 $(GeV/c)^2$ with ^{12}C target. Cross sections will be measured at two ω points below and three above the quasielastic peak, with the ones above covering the dip and the Δ region. Again, the whole missing energy spectrum at each point will be covered. The kinematics for ω dependence study is also shown on Table 1.

For the p and the s shells in ^{12}C, where energy resolution is important, we will have 2 MeV E_m bins. To achieve good energy resolution, we will use thin (0.1 g/cm^2) targets. With a beam current of 100 μA, this corresponds to a luminosity of $\sim 10^{37}$ $cm^{-2}sec^{-1}$ for $^{3,4}He$ and $\sim 0.3 \times 10^{37}$ $cm^{-2}sec^{-1}$ for ^{12}C. At high missing energies ($E_m > 80$ MeV), the cross sections are expected to be much lower. However since there is no narrow shell structure in this region, good energy resolution is not necessary. We will increase the size of the missing energy bins to increase statistics. Also to increase statistics, we will use a thicker ^{12}C target (0.4 g/cm^2). For ^3He and ^4He, since the cross sections are not as low at our kinematics, we will not increase the target thickness.

For all of the above measurements, we will have statistics of about 1% for each E_m bin at the p shell and the peak of the s shell. For the tails of the s shell and the higher missing energy continuum, we will collect data at each E_m bin for approximately the same length of time as for the bin at the peak of the s shell, with expected statistics of about $2\% - 5\%$.

Table 3 gives counting rate estimates derived using the computer code MCEEP[31]. The simulation includes effects such as averaging over finite acceptances and non-uniform weighting for the variation in cross sections. In the calculation, we assumed the following

Table 1

Kinematics for ^{12}C							
Kin. #	Q^2 $(GeV/c)^2$	q (GeV/c)	ω (GeV)	E_i (GeV)	E_f (GeV)	θ_e (degrees)	θ_q (degrees)
1(f)	0.2	0.466	0.132	1.725	1.593	15.5	-66.00
1(b)	0.2	0.466	0.132	0.389	0.257	90.0	-33.47
2(f)	0.6	0.848	0.345	3.050	2.705	15.5	-58.48
2(b)	0.6	0.848	0.345	0.747	0.402	90.0	-28.30
3(f)	1.0	1.145	0.558	4.000	3.442	15.5	-53.45
3(b)	1.0	1.145	0.558	1.039	0.481	90.0	-24.84
4(f)	1.5	1.476	0.824	4.000	3.176	19.8	-46.79
4(b)	1.5	1.476	0.824	1.371	0.547	90.0	-21.75
5	1.0	1.062	0.358	4.000	3.642	15.5	-66.41
6	1.0	1.100	0.458	4.000	3.542	15.5	-59.37
7	1.0	1.197	0.658	4.000	3.342	15.5	-48.26
8	1.0	1.255	0.758	4.000	3.242	15.5	-43.66
9	1.0	1.318	0.858	4.000	3.142	15.5	-39.57

Table 2

Kinematics for ^{3,4}He							
Kin. #	Q^2 $(GeV/c)^2$	q (GeV/c)	ω (GeV)	E_i (GeV)	E_f (GeV)	θ_e (degrees)	θ_q (degrees)
^{3}He(f)	1.0	1.145	0.558	4.000	3.442	15.5	-53.45
^{3}He(b)	1.0	1.145	0.558	1.039	0.481	90.0	-24.84
^{4}He(f)	1.0	1.145	0.558	4.000	3.442	15.5	-53.45
^{4}He(b)	1.0	1.145	0.558	1.039	0.481	90.0	-24.84

conditions: a) Each spectrometer has 10% momentum acceptance and 7.8 msr solid angle; b) Beam current is 100 μA; c) ^{12}C targets thicknesses are 0.1 and 0.4 g/cm^2; d) Both 10 cm long gas ^{3}He and ^{4}He targets have thickness of 0.1 g/cm^2. To include the missing energy dependence, we used existing (e,e'p) data [13,18,19] to extrapolate to our kinematics.

Single rates for (e,e') and (e,p) were calculated using the computer codes QFS and EPC[32]. Figures 7 and 8 show the typical single (e,e') and (e,p) cross sections for our kinematics. From these single rates, accidental rates were calculated assuming 1 ns timing resolution. These calculations were checked with existing data at some appropriate kinematics. Signal to noise ratios were estimated and are also listed in table 3. Only at a few kinematical points at the extreme high missing energy, do the signal to noise ratios become a concern.

To estimate background contamination, we used the computer code EPC to estimate the total π^- and π^+ contributions in the electron and proton spectrometers, respectively (also shown in figures 7 to 10). The π^+ contributions in the proton spectrometer are all small. The maximum π^+ to proton ratio is less than 1, which can be easily handled. The π^- contributions in the electron spectrometer can be large. The π^- to electron ratio is mostly less than 30, except for the highest Q^2 at backward angle where it is $\sim$ 100. With a π^- rejection rate of 10^4 (design goal is 10^6), this will contribute less than 1%. We also checked the coincidence background by using the existing (e,e'p) and (e,π^-p) data, and found the ratio of cross sections from (e,π^-p) to that from (e,e'p) is again less than 30. It should present no problem.

IV. SUMMARY

The experiment proposed here will probe, at selected kinematics with ^{12}C and ^{3}He, ^{4}He, the nature of the (e,e'p) and (e,e') reactions including possible multinucleon processes at high missing energy. CEBAF provides the best facility to study (e,e'N) reactions in nuclear physics. The Hall A high resolution, high precision capability enables us to perform R_L, R_T separations to high momentum transfers and at deep missing energies. These proposed measurements can greatly add to our understanding of nucleon-nucleon interactions and correlations as well as the possible nuclear medium effects on the nucleons. The beam time requested for this experiment is 720 hours.

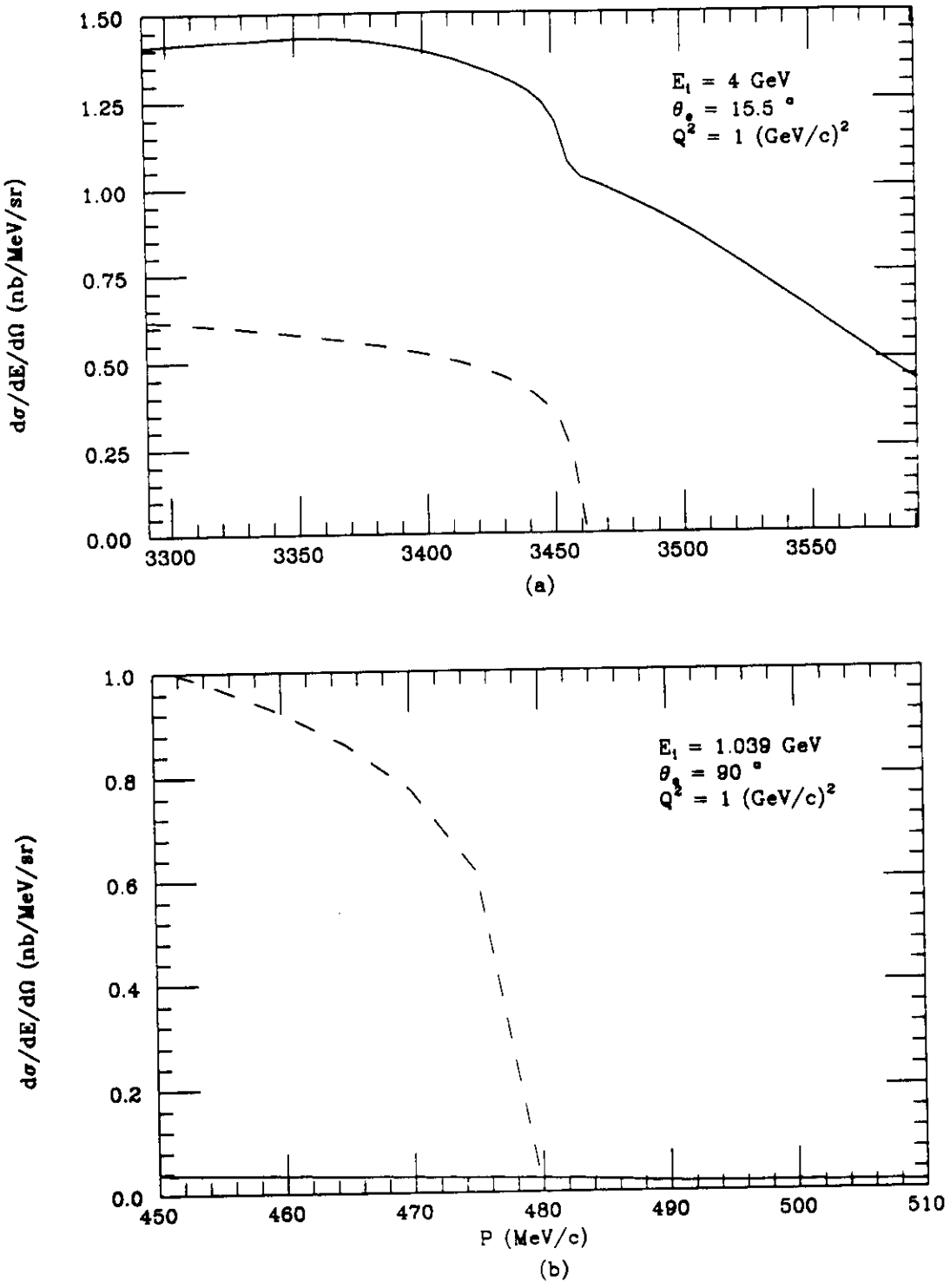

Figure 7. Single (e,e') and (e,π^-) cross sections at $Q^2 = 1(GeV/c)^2$ for forward (a) and backward (b) angles. Solid curves are for (e,e') and dashed curves for (e,π^-).

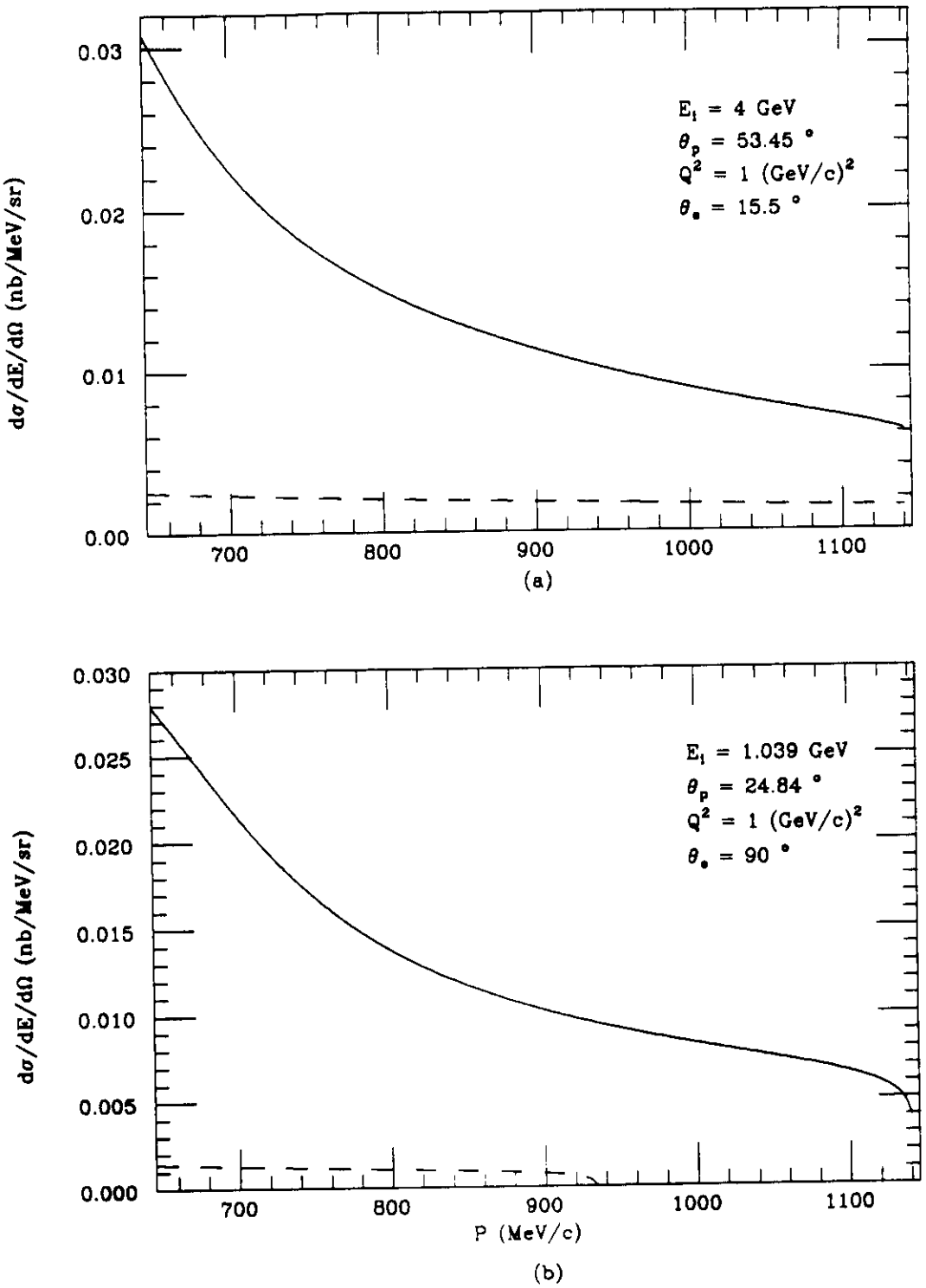

Figure 8. Single (e,p) and (e,π^+) cross sections at $Q^2 = 1(GeV/c)^2$ for forward (a) and backward (b) angles. Solid curves are for (e,p) and dashed curves for (e,π^+).

Table 3

Counting Rate							
Target	Kin. #	Q^2 $(GeV/c)^2$	θ_e (degrees)	ω (GeV)	(*) σ $(nb/MeV/sr^2)$	(*) Rate 1/sec.	Time (hours)
^{12}C	1(f)	0.2	15.5	0.132	94	221	2
^{12}C	1(b)	0.2	90.0	0.132	2.5	1.7	85
^{12}C	2(f)	0.6	15.5	0.345	13.6	90.4	3
^{12}C	2(b)	0.6	90.0	0.345	0.58	1.8	64
^{12}C	3(f)	1.0	15.5	0.558	3.6	37.9	6
^{12}C	3(b)	1.0	90.0	0.558	0.19	0.97	109
^{12}C	4(f)	1.5	19.8	0.824	0.79	11.6	13
^{12}C	4(b)	1.5	90.0	0.824	0.063	0.44	207
^{12}C	5	1.0	15.5	0.358	0.20	1.3	19
^{12}C	6	1.0	15.5	0.458	1.69	16.9	3
^{12}C	7	1.0	15.5	0.658	2.87	32.5	6
^{12}C	8	1.0	15.5	0.758	1.22	14.6	6
^{12}C	9	1.0	15.5	0.858	0.37	3.2	19
^{4}He	(f)	1.0	15.5	0.558	7.3	231	3
^{4}He	(b)	1.0	90.0	0.558	0.39	6.6	68
^{3}He	(f)	1.0	15.5	0.558	9.4	394	3
^{3}He	(b)	1.0	90.0	0.558	0.83	18.8	30
7 Energy, 6 Spectrometer Angle Changes							74
Total Beam Time							720

(*) σ and Rate are for S shell only details see tables 4 to 10

Table 4–1(f)

Counting Rate and Signal to Noise Ratio at Kin.1(f)							
P_r (MeV/c)	E_m (MeV)	I×t μA g/cm^2	R_a sec^{-1}	R_c sec^{-1}	S/N	Bin Size (MeV)	Time (hours)
466	23	10	14	88	6.3	2	0.2
429	39	10	15	155	10	2	0.2
394	52	10	18	55	3.0	2	0.3
363	64	10	22	11	0.5	2	0.5
334	74	10	29	4.5	0.16	4	0.5
Subtotal Time							1.7

Table 4–1(b)

Counting Rate and Signal to Noise Ratio at Kin.1(b)							
P_r (MeV/c)	E_m (MeV)	I×t μA g/cm^2	R_a sec^{-1}	R_c sec^{-1}	S/N	Bin Size (MeV)	Time (hours)
466	23	10	0.033	0.35	11	2	20
429	39	10	0.056	1.17	21	2	15
394	52	10	0.075	0.42	5.6	2	20
363	64	20	0.37	0.17	0.46	4	16
334	74	20	0.45	0.067	0.15	8	14
Subtotal Time							83

Table 4–2(f)

Counting Rate and Signal to Noise Ratio at Kin.2(f)							
P_r (MeV/c)	E_m (MeV)	I×t μA g/cm^2	R_a sec^{-1}	R_c sec^{-1}	S/N	Bin Size (MeV)	Time (hours)
848	19	10	0.67	76	110	2	0.2
780	63	10	0.74	90	120	2	0.5
718	102	40	0.91	12	13	4	0.6
660	136	40	1.2	8.0	6.7	8	0.4
608	166	40	1.5	5.5	3.4	10	0.3
559	191	40	1.8	2.7	1.5	15	0.2
514	213	40	1.8	2.4	1.3	15	0.2
473	232	40	1.8	1.6	0.89	20	0.2
Subtotal Time							2.6

Table 4–2(b)

Counting Rate and Signal to Noise Ratio at Kin.2(b)							
P_r (MeV/c)	E_m (MeV)	I×t μA g/cm^2	R_a sec^{-1}	R_c sec^{-1}	S/N	Bin Size (MeV)	Time (hours)
848	19	10	0.0020	0.53	268	2	20
780	63	10	0.0025	1.8	730	2	20
718	102	40	0.049	0.96	20	4	7
660	136	40	0.060	0.64	11	8	5
608	166	40	0.067	0.44	6.6	10	4
559	191	40	0.068	0.20	2.9	15	3
514	213	40	0.072	0.18	2.5	15	3
473	232	40	0.089	0.12	1.3	20	2
Subtotal Time							64

Table 4–3(f)

Counting Rate and Signal to Noise Ratio at Kin.3(f)							
P_r (MeV/c)	E_m (MeV)	I×t μA g/cm^2	R_a sec^{-1}	R_c sec^{-1}	S/N	Bin Size (MeV)	Time (hours)
1145	16	10	0.16	68	423	2	1.0
1053	86	10	0.17	11	66	4	1.1
969	147	10	0.19	3.1	10	8	1.0
892	202	40	0.22	1.5	7.0	10	0.9
820	250	40	0.24	0.76	3.1	15	1.0
755	292	40	0.28	0.38	1.4	20	1.1
Subtotal Time							6.1

Table 4–3(b)

Counting Rate and Signal to Noise Ratio at Kin.3(b)							
P_r (MeV/c)	E_m (MeV)	I×t μA g/cm^2	R_a sec^{-1}	R_c sec^{-1}	S/N	Bin Size (MeV)	Time (hours)
1145	16	10	0.00043	1.0	2300	2	56
1053	86	40	0.0080	1.2	150	4	11
969	147	40	0.0084	0.32	37	8	12
892	202	40	0.0096	0.16	17	10	10
820	250	40	0.011	0.08	7	15	10
755	292	40	0.013	0.04	3	20	10
Subtotal Time							109

Table 4–4(f)

Counting Rate and Signal to Noise Ratio at Kin.4(f)							
P_r (MeV/c)	E_m (MeV)	I×t μA g/cm^2	R_a sec^{-1}	R_c sec^{-1}	S/N	Bin Size (MeV)	Time (hours)
1476	13	10	0.021	19.3	940	2	3.5
1358	112	10	0.022	4.6	210	4	4.0
1249	200	10	0.025	0.58	24	10	3.8
1149	279	10	0.027	0.35	13	20	1.6
Subtotal Time							12.9

Table 4–4(b)

Counting Rate and Signal to Noise Ratio at Kin.4(b)							
P_r (MeV/c)	E_m (MeV)	I×t μA g/cm^2	R_a sec^{-1}	R_c sec^{-1}	S/N	Bin Size (MeV)	Time (hours)
1476	13	10	0.00014	0.42	3000	2	140
1358	112	40	0.0026	0.65	250	4	28
1249	200	40	0.0027	0.082	30	10	27
1149	279	40	0.0029	0.049	17	20	12
Subtotal Time							209

Table 4–^{4}He(f)

Counting Rate and Signal to Noise Ratio at Kin.^{4}He(f)							
P_r (MeV/c)	E_m (MeV)	I×t μA g/cm^2	R_a sec^{-1}	R_c sec^{-1}	S/N	Bin Size (MeV)	Time (hours)
1145	16	10	0.012	116	10000	2	0.8
1053	86	10	0.017	104.1	6000	3	0.4
969	147	10	0.019	11.6	610	5	0.3
892	202	10	0.020	2.3	110	10	0.6
820	250	10	0.023	1.2	45	15	0.9
Subtotal Time							3.0

Table 4–^{4}He(b)

Counting Rate and Signal to Noise Ratio at Kin.^{4}He(b)							
P_r (MeV/c)	E_m (MeV)	I×t μA g/cm^2	R_a sec^{-1}	R_c sec^{-1}	S/N	Bin Size (MeV)	Time (hours)
1145	16	10	0.000030	3.3	110000	2	27
1053	86	10	0.000058	3.0	51000	3	15
969	147	10	0.000063	0.33	5200	5	8
892	202	10	0.000071	0.066	930	10	10
820	250	10	0.000080	0.033	410	15	8
Subtotal Time							68

Table 4–^{3}He(f)

Counting Rate and Signal to Noise Ratio at Kin.^{3}He(f)							
P_r (MeV/c)	E_m (MeV)	I×t μA g/cm^2	R_a sec^{-1}	R_c sec^{-1}	S/N	Bin Size (MeV)	Time (hours)
1145	16	10	0.0091	237	26000	2	0.4
1053	86	10	0.013	146	11000	3	0.4
969	147	10	0.014	11.8	820	5	0.9
892	202	10	0.015	3.9	270	10	0.5
820	250	10	0.023	2.0	130	15	0.4
Subtotal Time							2.6

Table 4–^{3}He(b)

Counting Rate and Signal to Noise Ratio at Kin.^{3}He(b)							
P_r (MeV/c)	E_m (MeV)	I×t μA g/cm^2	R_a sec^{-1}	R_c sec^{-1}	S/N	Bin Size (MeV)	Time (hours)
1145	16	10	0.000026	11.3	440000	2	8
1053	86	10	0.000051	6.9	130000	3	7
969	147	10	0.000056	0.56	10000	5	5
892	202	10	0.000062	0.19	3000	10	6
820	250	10	0.000073	0.094	1300	15	4
Subtotal Time							30

REFERENCES

[1] J. S. O'Connell *et al.*, Phys. Rev. Lett. **53**, 1627 (1984); Phys. Rev. **C35**, 1063 (1987).

[2] R. R. Whitney *et al.*, Phys. Rev. **C9**, 2230(1974).

[3] W. van Orden and T. W. Donnelly, Ann. Phys. **131**, 451 (1981).

[4] J. M. Finn, R. W. Lourie and B. H. Cottman, Phys. Rev. **C29**, 2230 (1984).

[5] A. Magnon, Saclay; private communication.

[6] J. P. Chen *et al.*, Phys. Rev. Lett. **66**, 1283 (1991).

[7] Z. E. Meziani *et al.*, Phys. Rev. Lett. **69**, 41 (1992).

[8] P. Barreau *et al.*, Nucl. Phys. **A402**, 515 (1983); Z. E. Meziani *et al.*, Phys. Rev. Lett., **52**, 2130 (1984).

[9] G. Do Dang and N. van Giai, Phys. Rev. **C30**, 731 (1984).

[10] C. R. Chinn *et al.*, Phys. Rev. **C40**, 790 (1989).

[11] X. Song, J. Chen, J. McCarthy, Z. Phys **A341**, 275 (1992); J. Phys. **G17**, L75 (1991).

[12] L. Celenza *et al.*, Phys. Rev. **C33**, 1012 (1986).

[13] P. E. Ulmer *et al.*, Phys. Rev. Lett. **59**, 2259 (1987).

[14] G. van der Steenhoven *et al.*, Nucl. Phys. **A480**, 547 (1988).

[15] J. B. J. M. Lanen *et al.*, Phys. Rev. Lett. **64**, 2250 (1990).

[16] R. W. Lourie *et al.*, Phys. Rev. Lett. **56**, 2364 (1986).

[17] H. Baghaei *et al.*, Phys. Rev. **C39**, 177 (1989).

[18] L. B. Weinstein *et al.*, Phys. Rev. Lett. **64**, 1646 (1990).

[19] J. Morrison *et al.*, to be published.

[20] S. Penn *et al.*, to be published.

[21] C. Marchand *et al.*, Phys. Rev. Lett. **60**, 1703 (1988).

[22] J. L. Friar, Modern Topics in Electron Scattering, ed. B. Frois and I. Sick, World Scientific, Singapore (1991).

[23] J. Strate *et al.*, J. Phys. **G14**, 229 (1988); Nucl. Phys. **A501**, 51 (1989).

[24] G. Backenstoss *et al.*, Phys. Rev. Lett. **55**, 2782 (1985).

[25] C. H. Q. Ingram, Nucl. Phys. **A553**, 573c (1993).

[26] P. Weber *et al.*, Phys. Rev. **C43**, 1553 (1991).

[27] B. L. Berman, proceedings of the European Workshop on Few-Body Physics, Few Body Sys. Supp. 1, ed. C. Ciofi degli Atti *et al.*, Springer-Verlag, New York, 541 (1986).

[28] G. Audit *et al.*, Phys. Rev. **C44**, 575 (1991).

[29] A. J. Sarty *et al.*, Phys. Rev. **C47**, 459 (1993).

[30] J. M. Laget, J. Phys. **G14**, 1445 (1988).
[31] P. E. Ulmer, Computer code MCEEP.
[32] J. Lightbody, J. O'Connell, Comp. in Phys. **Vol. 2**, 57 (1988).